

Magnesium Ion-Conducting Biopolymer Electrolytes Based on Carboxymethyl Cellulose Derived from Palm Oil Empty Fruit Bunch Fibre

M.S.A. Rani^{1,2,*}, N.S. Isa³, M.H. Sainorudin¹, N.A. Abdullah¹, M. Mohammad^{1*}, N. Asim¹, H. Razali¹, M.A. Ibrahim¹

¹ Solar Energy Research Institute (SERI), Universiti Kebangsaan Malaysia, 43600 Bangi, Selangor, Malaysia

² Research Centre for Tropicalisation, National Defence University of Malaysia, Sungai Besi Camp, 57000 Kuala Lumpur, Malaysia

³ Jabatan Agroteknologi dan Bio-industri, Kolej Komuniti Rembau, 71400 Rembau, Negeri Sembilan, Malaysia

*E-mail: iker.asmal55@gmail.com; masita@ukm.edu.my

Received: 5 October 2020 / Accepted: 29 November 2020 / Published: 31 January 2021

As demands for global lithium supplies have raised questions about the sustainability of the supply of lithium, a potential alternative to lithium batteries has been developed. New biodegradable-carboxymethyl cellulose (CMC) extracted from empty fruit bunches of palm oil is used to produce biopolymer electrolytes (BPE) using magnesium acetate salt. Solution casting has been used to prepare biopolymer electrolytes in various ratios of magnesium acetate. Via Fourier transform infrared characterisation, electrochemical impedance spectroscopy, transference number measurements and linear sweep voltammetry, studies on the structural, electrical and electrochemical behaviour of CMC were conducted. Upon the addition of 20 wt% of magnesium acetate, the highest ionic conductivity of $1.83 \times 10^{-3} \text{ S cm}^{-1}$ at ambient temperature was achieved. The interactions between CMC and magnesium acetate were verified by the Fourier transform infrared results. Electrochemical stability of more than 2 V was shown by the biosourced polymer electrolytes, whereas the measurement of transference number showed that electrolytic conduction was dominated by ions.

Keywords: carboxymethyl cellulose; biosourced polymer electrolytes; magnesium acetate; electrical studies

1. INTRODUCTION

With the current demand for supplies of renewable energy, the construction and optimisation of energy storage systems are becoming increasingly important. At present, Li⁺ ion batteries have attracted the attention of researchers because of the small ionic Li⁺ ion radii that can be intercalated across the

layers of electrode-layered materials [1]. Concerns over the availability of lithium, although often costly, have emerged with the possibility of immense demands on sufficient global lithium supplies [6, 7]. Many global reserves of lithium are found in remote or politically sensitive areas [2, 3]. Although robust systems for battery recycling are developed, recycling may not be able to avoid this resource depletion in time [4]. In addition, the increased use of lithium in medium-scale car batteries will increase the price of lithium compounds, making large-scale storage prohibitively costly [5]. Therefore, analysis must be conducted to investigate alternative sources of charge carriers to replace Li^+ . Various polymer electrolytes based on lithium have been documented by several research groups for display in the battery systems. Therefore, in order to replace Li^+ , the aim of the extended study is to explore alternative sources of charge carriers. Compared with lithium salts, magnesium salts show great potential because of its properties, which will be impregnated in carboxymethyl cellulose (CMC) from palm oil empty fruit bunch.

However, the use of rechargeable lithium batteries, is hindered by their safety drawbacks (highly reactive in nature and simple organic electrolyte burning and explosion) and high costs, which are the main factors in designing batteries. Therefore, given its low cost, non-toxicity, abundance and environmentally safe materials, magnesium may be a potential alternative to lithium for aqueous rechargeable batteries to address these limitations [8, 9]. The magnesium-based rechargeable battery systems have recently gained attention because of their performance capabilities; they are predicted to be similar to those of rechargeable lithium-based batteries [9-13]. Consequently, the production of electrolyte-conducting magnesium ion has become a significant problem in achieving rechargeable magnesium, in which a solid polymer electrolyte is an important component. Given the following advantages, materials exhibiting Mg^{2+} conductivity are important: (1) 68 and 65 pm are the ionic radii of Li^+ and Mg^{2+} , respectively, that is, equal in magnitude. Therefore, the probability of replacing Li^+ ions with Mg^{2+} ions in insertion compounds is possible. (2) Magnesium is a more stable metal than lithium. Unlike lithium, which requires high-purity argon or helium atmosphere, magnesium can be safely treated in oxygen and humid atmospheres. Therefore, magnesium metal-related safety issues are limited. (3) Global magnesium supplies are abundant in raw materials and are cheaper than lithium [14].

However, the use of magnesium complexed electrolyte films has been found to exhibit several advantages over their lithium counterparts. The interaction between Li^+ ion and the polar groups of polymer is stronger than that of Mg^{2+} ion [15]. Thus, Li^+ ion transfer requires higher activation energy than Mg^{2+} ion in polymer electrolytes [16]. Magnesium provides a compelling rationale for the study of the polymer battery systems, which is another alternative system, because of its low cost, natural abundance, low toxicity, low atomic mass and high enough electrochemical reduction potential. In view of negligible hazard and enhanced safety, studies of rechargeable magnesium batteries must be further studied.

Despite the considerable research on biopolymer electrolytes, no work has been conducted on the interaction of CMC synthesised from palm oil empty fruit bunch fibre with the magnesium acetate biopolymer electrolyte system. In view of the afore-mentioned discussion, the interactions and electrical and electrochemical properties of CMC- $\text{Mg}(\text{CH}_3\text{COO})_2$ biopolymer electrolytes are investigated by various physical techniques, namely, infrared spectroscopy, complex impedance analysis, linear sweep voltammetry and transport number measurements.

2. EXPERIMENTAL

2.1. Biopolymer electrolyte preparation

CMC derived from palm oil empty fruit bundle was commercially obtained from Sabah Softwoods Sdn. Bhd., Malaysia, whereas $\text{Mg}(\text{CH}_3\text{COO})_2$ was bought from Sigma-Aldrich, Germany. Both products have been used without further purification. The CMC used in the present work was derived from palm oil empty fruit bunches and cellulose isolation, and its derivation followed the process used in our previous paper [17]. The degree of substitution (DS) of CMC was 1.15 which was higher than that of commercial CMCs. Therefore, CMC had a high number of oxygen and active sites for coordination with doping salt cations, thereby resulting in a high conductivity value [17]. All BPE films have been prepared using solution casting. A pure CMC (without salt) film has also been prepared as a reference sample. Sufficient amounts of CMC and doping salts were dissolved in 40 mL of aqueous acetic acid (1 %) solution at room temperature for the preparation of BPE films. Homogeneous solution was obtained after several hours of stirring using a magnetic stirrer. The final clear solution was then casted onto Petri dishes and left to dry at room temperature to form highly translucent and flexible thin films. The films were placed in a desiccator for further drying. The composition of BPE films and their designation are shown in Table 1.

Table 1. Designation of BPE films

Composition (CMC: $\text{Mg}(\text{CH}_3\text{COO})_2$) (wt%)	Designation
100 : 0	CMC-Mg(0)
90 : 10	CMC-Mg(10)
80 : 20	CMC-Mg(20)
70 : 30	CMC-Mg(30)
60 : 40	CMC-Mg(40)

2.2. Biopolymer electrolyte characterization

Fourier Transform Infrared (FTIR) spectroscopy was performed to investigate the interactions between CMC and $\text{Mg}(\text{CH}_3\text{COO})_2$. FTIR was performed using a Perkin Elmer Frontier FTIR spectrometer fitted with an attenuated complete reflecting adapter. The sample was placed on the top of the diamond surface with a pressure applied to the sample, and the infrared light was transmitted through the sample. FTIR spectra have been reported in the spectral range from 4000 cm^{-1} to 500 cm^{-1} at a resolution of 2 cm^{-1} . The FTIR data were recorded in the transmittance mode. Electrical analysis was performed using a Solartron 1260 impedance/gain phase analyser with a frequency between 10 and 4 MHz. Each BPE sample was sandwiched between two stainless steel electrodes with a diameter of 2.0 cm (area = 3.142 cm^2). The impedance of the samples was measured between 303 K and 338 K. Ionic

transference number was calculated using direct current polarisation by monitoring the polarisation current as a function of time. The BPE films were sandwiched between two stainless steel blocking electrodes connected to a 1.5 V voltage source. The electrochemical stability window of the electrolytes (the selected BPE) was calculated using linear sweep voltammetry (LSV) performed on the Wonatech ZIVE MP2 multichannel electrochemical workstation. LSV was performed using stainless steel electrodes at a scanning rate of 1 mVs^{-1} from 0 V to 4 V.

3. RESULTS AND DISCUSSION

3.1. FTIR spectroscopy analysis

The FTIR spectra of $\text{Mg}(\text{CH}_3\text{COO})_2$, pure CMC as reference and CMC-Mg(0-40) in the region from 550 cm^{-1} to 4000 cm^{-1} are shown in Figure 1. The hydroxyl band for pure CMC (Figure 1 [b]) appears at 3347 cm^{-1} . As the $\text{Mg}(\text{CH}_3\text{COO})_2$ concentration increases, the hydroxyl band shifts to a lower wavenumber. This finding indicates the interaction of the cation $[\text{Mg}^{2+}]$ substructure of $\text{Mg}(\text{CH}_3\text{COO})_2$ with oxygen atoms of the hydroxyl group of CMC [18]. Although the interaction between the polymer host and ionic salt normally occurs at the oxygen atom, other bands can also be affected [19]. Upon addition of 20 wt% of $\text{Mg}(\text{CH}_3\text{COO})_2$, the carboxyl group ($\text{C}=\text{O}$) at 1597 cm^{-1} has shifted to a lower wavenumber (1557 cm^{-1}), which indicates the interaction of the ($\text{C}=\text{O}$) moiety in CMC with Mg^{2+} . This phenomenon can be related to the lone pair electrons that have attracted the salt molecule of $\text{Mg}(\text{CH}_3\text{COO})_2$ to the system [20]. The concentration of Mg^{2+} increases with the increase of $\text{Mg}(\text{CH}_3\text{COO})_2$ composition, implying that more electrons are withdrawn towards $\text{C}=\text{O}$, which lead to the shift of band from 1557 cm^{-1} to 1549 cm^{-1} .

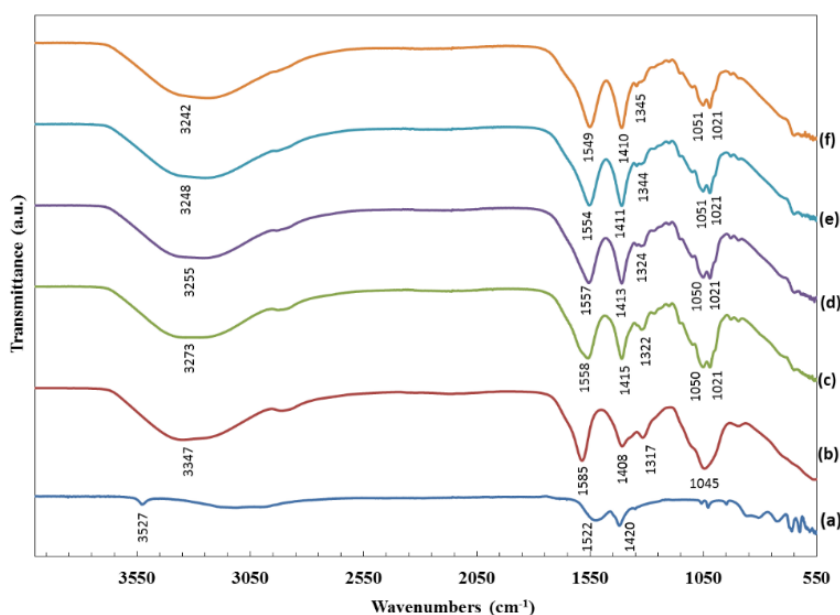


Figure 1. IR-spectra of (a) $\text{Mg}(\text{CH}_3\text{COO})_2$, (b) CMC powder, (c) CMC-Mg(10), (d) CMC-Mg(20), (e) CMC-Mg(30) and (f) CMC-Mg(40) in the spectral region between 4000 and 550 cm^{-1} .

3.2. Electrochemical impedance spectroscopy analysis

3.2.1. Ionic conductivity

Figure 2 shows typical complex impedance spectra for the BPE film of the CMC-Mg(20) system at different temperatures. No semicircle is found in this complex impedance plot, thereby indicating the remaining resistive component of the BPEs [21]. The impedance spectra show a low frequency spike, indicating that the conduction is due to ions. In addition, the inclined spikes at less than 90° to the actual impedance axis obtained in this work can be clarified by the roughness of the electrode-electrolyte interface [22, 23]. As shown in Figure 2, bulk resistance decreases with temperature because of an increase in the number of charge carriers and their mobility with temperature [24, 25].

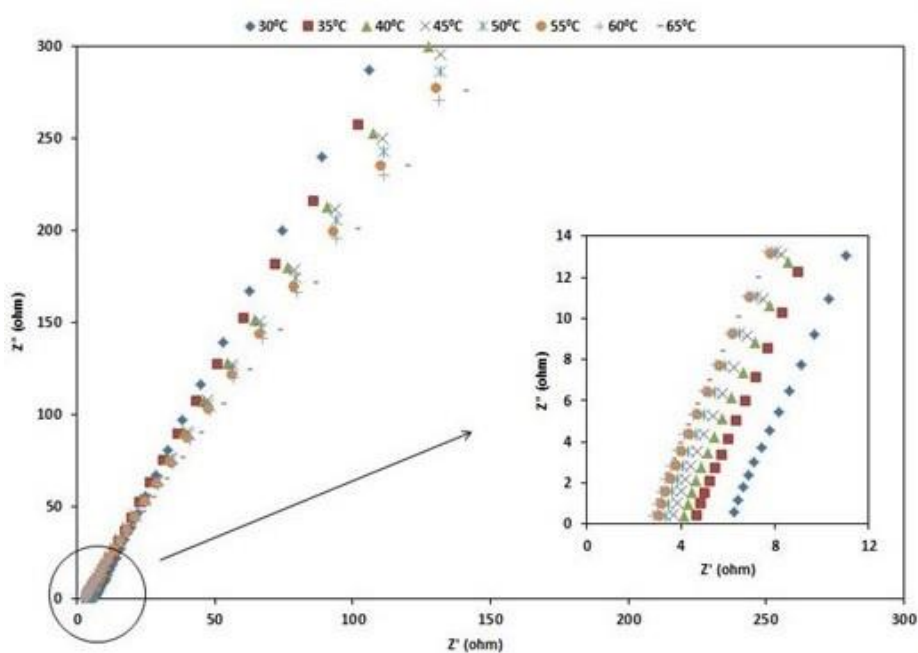


Figure 2. Complex impedance spectra for CMC added with 20 wt% $\text{Mg}(\text{CH}_3\text{COO})_2$ films at different temperatures.

Figure 3 shows room-temperature conductivity as a function of the wt% of $\text{Mg}(\text{CH}_3\text{COO})_2$. The conductivity ascends with the increase in salt concentration until it reaches a maximum value of $1.83 \times 10^{-3} \text{ S cm}^{-1}$ at 20 wt% of $\text{Mg}(\text{CH}_3\text{COO})_2$ and decreases slowly with the further increase in $\text{Mg}(\text{CH}_3\text{COO})_2$ content. The improved ionic conductivity can be attributed to the number of charge carriers. Buraidah and co-researchers [26] reported that the aggregation of ions impeded the movement of mobile ions resulting in a decrease in ionic conductivity. A similar trend was reported by Mobarak and co-workers [27]. The highest conductivity of the carboxymethyl iota carrageenan and carboxymethyl kappa carrageenan doped lithium nitrate biopolymer electrolyte achieved by these researchers were $5.85 \times 10^{-3} \text{ S cm}^{-1}$ and $5.51 \times 10^{-3} \text{ S cm}^{-1}$, respectively. The high conductivity value obtained in this work indicates that the conductivity of BPE can be enhanced by using the derivatives of cellulose.

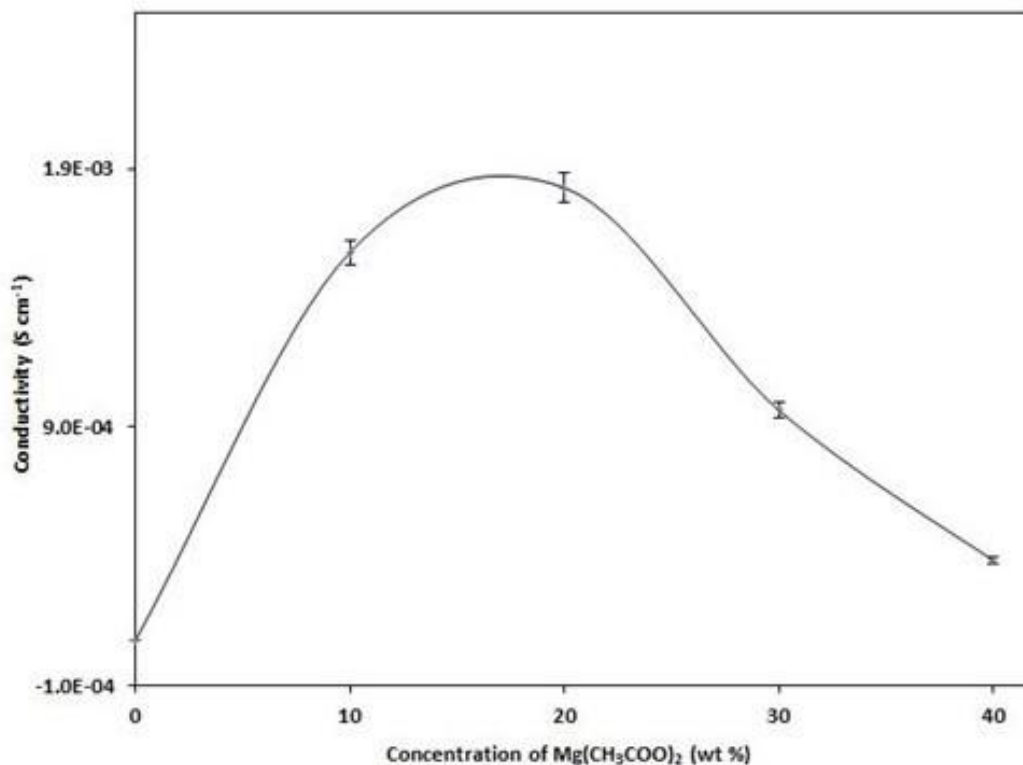


Figure 3. Room-temperature conductivity as a function of the Mg(CH₃COO)₂ content (0 wt% to 40 wt%).

The drop in conductivity for films containing more than 20 wt% of Mg(CH₃COO)₂ is attributed to the host matrix, which is packed with ions (overcrowding), thereby resulting in limited charge carrier mobility [28]. For this study, the amount of Mg(CH₃COO)₂ is limited to 40 wt% because the biopolymer films containing more than this amount suffered from poor mechanical stability.

3.2.2. Temperature-dependent ionic conductivity

The variations of conductivity with temperature for the samples of CMC-Mg(CH₃COO)₂ BPEs are presented in Figure 4. The conductivity of both BPEs shows an increasing trend with the increase in temperature, which is ascribed to the increase in the number of density and mobility of ions [29, 30]. All the points of each plot in Figure 4 lie on a straight line and the regression value is approximately 1. The linear relationship indicates that the biopolymer system follows the Arrhenius-type thermally activated process.

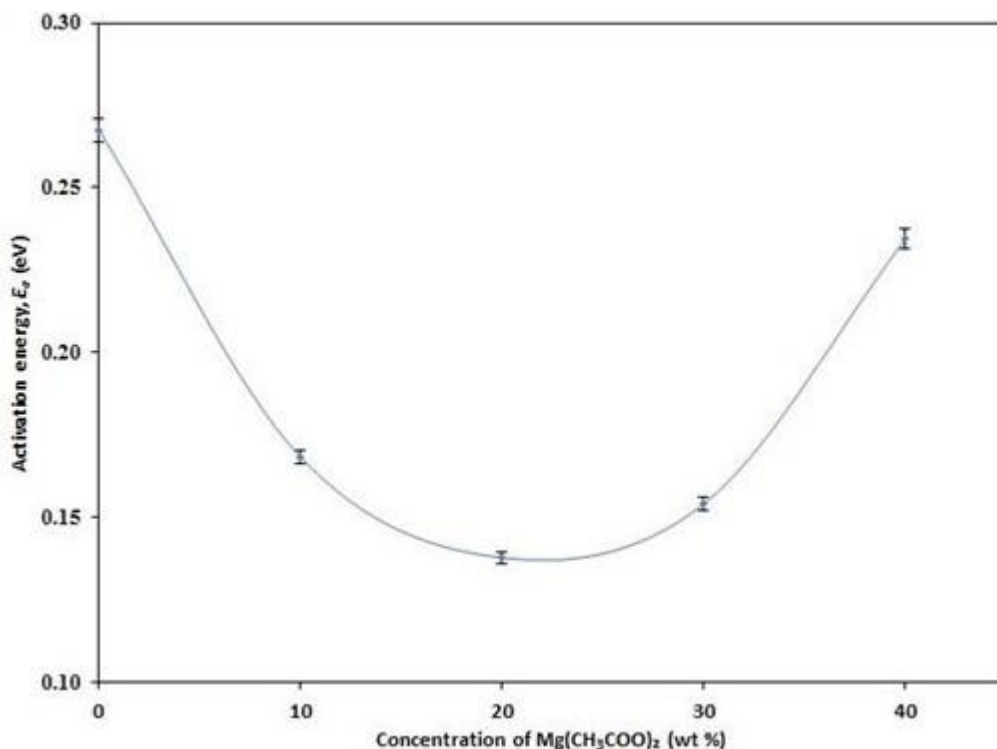


Figure 4. Activation energy versus the concentration of CMC-Mg(CH₃COO)₂ (0 wt%-40 wt%).

Figure 4 shows the plot of the activation energy versus concentration of Mg(CH₃COO)₂ (0 wt%-40 wt%). E_a is the energy required for an ion to migrate from one site to another. The BPE system has a low E_a value of 0.14 eV.

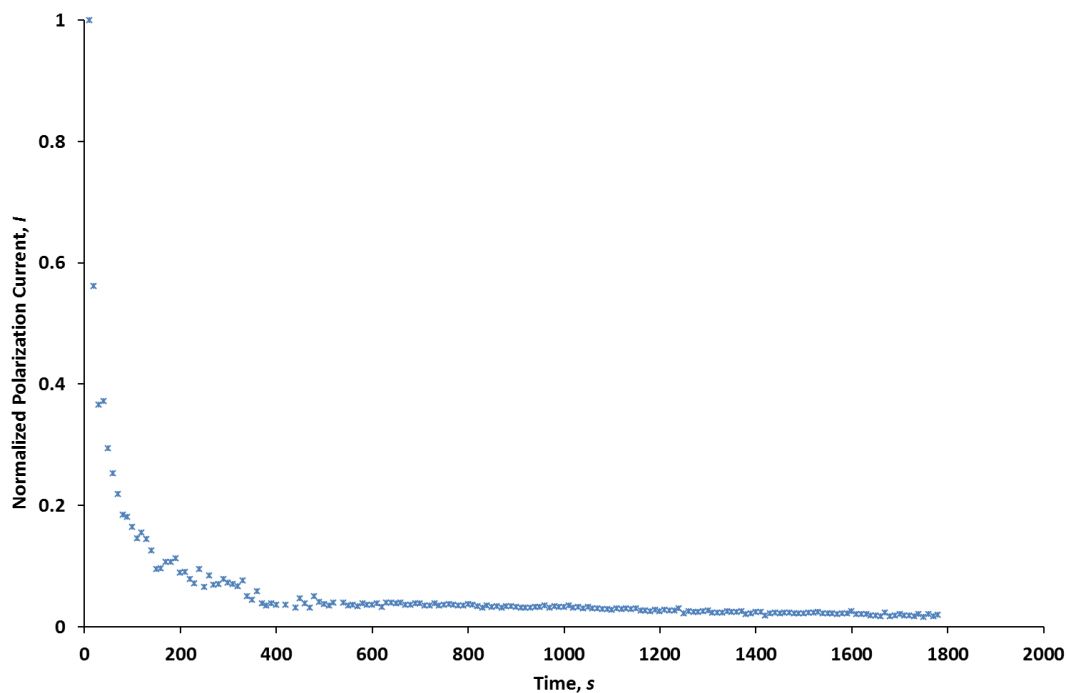


Figure 5. Normalised polarisation current versus time for the biopolymer film of CMC-Mg(20).

3.3. Ionic transference number measurements

The ionic transference number for the highest conducting system, CMC-Mg(20) is determined by using Wagner's polarisation method. In this technique, the direct current (DC) is monitored as a function of time on an application of a fixed DC voltage of 1.0 V across the SS/biopolymer electrolytes/SS. After polarisation, the graph of normalised current versus time was plotted. Figure 5 depicts the plot of the normalised polarisation current versus time for the CMC-Mg(20) system. The value of ionic transference number for this system is 0.98. This suggests that the charge transport in the CMC-Mg(20) is due to ions.

3.4. Electrochemical stability determination

The electrochemical stability window of electrolytes in this system was carried out by using LSV measurement. LSV is performed to determine the decomposition voltage of the electrolyte; the maximum operational voltage of an electrochemical device is stable, in which the electrolyte can be applied [31]. Figure 6 illustrates the LSV curve of the CMC-Mg(20) biopolymer electrolyte system. According to the work reported by Hamsan and co-researchers [32], a potential stability of 2.4 V has been obtained with the chitosan-magnesium acetate-glycerol system. The current increases gradually with the increase of voltage above 2.7 V (Figure 6). This voltage is the decomposition voltage of the studied sample, which indicates that the sample is stable enough to be applied as biopolymer electrolytes in electrochemical devices.

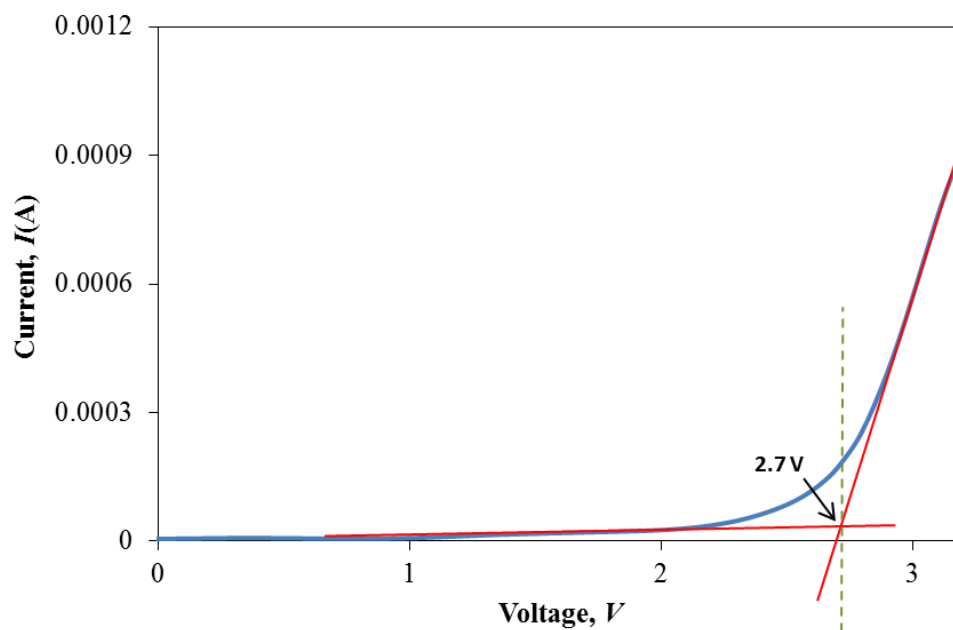


Figure 6. Linear sweep voltammetry curve for the biopolymer film of CMC-Mg(20).

4. CONCLUSION

The biopolymer electrolyte films of CMC extracted from palm oil empty fruit bunch prepared using magnesium acetate via solution casting. The optimised ionic conductivity was exhibited by the system containing 20 wt% of magnesium acetate of $1.83 \times 10^{-3} \text{ S cm}^{-1}$. Temperature-dependent ionic conductivity study revealed that the polymer electrolyte system followed the Arrhenius thermal-activated model. The FTIR study confirmed the interaction between the polymer hosts and acetate-based salts. Ionic transference number was found to be caused by ions. Linear sweep voltammetry results showed that the electrochemical stability of the magnesium acetate film was up to $\sim 2.9 \text{ V}$, indicating the suitability of BPEs for future practical applications in electrochemical devices.

ACKNOWLEDGMENTS

The authors would like to extend their gratitude towards the financial support from Centre of Research and Instrument Management, Universiti Kebangsaan Malaysia (MI-2019-018) and Malaysia's Ministry of Education through the Fundamental Research Grant Scheme (FRGS/1/2019/TK10/UKM/02/1).

References

1. M. S. A. Rani, M. Mohammad, M. S. Sua'it, A. Ahmad and N. S. Mohamed, *Polymer Bulletin*, (2020) 1.
2. F. Risacher and B. Fritz, *Aquatic Geochemistry*, 15 (2009) 123.
3. A. Yaksic and J. E. Tilton, *Resources Policy*, 34 (2009) 185.
4. B. L. Ellis and L. F. Nazar, *Current Opinion in Solid State and Materials Science*, 16 (2012) 168.
5. A. R. Polu and H.-W. Rhee, *Journal of Industrial and Engineering Chemistry*, 31 (2015) 323.
6. D. Larcher and J.-M. Tarascon, *Nature chemistry*, 7 (2015) 19.
7. W. Li, B. Song and A. Manthiram, *Chemical Society Reviews*, 46 (2017) 3006.
8. A. Guerfi, J. Trottier, I. Boyano, I. De Meazza, J. Blazquez, S. Brewer, K. Ryder, A. Vijn and K. Zaghbi, *Journal of Power Sources*, 248 (2014) 1099.
9. Y. Shao, N. N. Rajput, J. Hu, M. Hu, T. Liu, Z. Wei, M. Gu, X. Deng, S. Xu and K. S. Han, *Nano Energy*, 12 (2015) 750.
10. R. Manjuladevi, M. Thamilselvan, S. Selvasekarapandian, R. Mangalam, M. Premalatha and S. Monisha, *Solid State Ionics*, 308 (2017) 90.
11. K. Anilkumar, B. Jinisha, M. Manoj and S. Jayalekshmi, *European Polymer Journal*, 89 (2017) 249.
12. R. Deivanayagam, B. J. Ingram and R. Shahbazian-Yassar, *Energy Storage Materials*, 21 (2019) 136.
13. R. Deivanayagam, M. Cheng, M. Wang, V. Vasudevan, T. Foroozan, N. V. Medhekar and R. Shahbazian-Yassar, *ACS Applied Energy Materials*, 2 (2019) 7980.
14. R. Gamal, E. Sheha, N. Shash and M. G. El-Shaarawy, *Materials Express*, 4 (2014) 293.
15. Z.A. Halim, S. B. R. S. Adnan and N. S. Mohamed, *Ceramics International*, 42 (2016) 4452.
16. M. Mustafa, M.S.A. Rani, S. B. R. S. Adnan, F.M. Salleh and N. S. Mohamed, *Ceramics International*, 46 (2020) 28145.
17. M. S. A. Rani, S. Rudhzhiah, A. Ahmad and N. S. Mohamed, *Polymers*, 6 (2014) 2371.
18. A. K. Tiwari, M. Sowmiya and S. K. Saha, *Journal of Molecular Liquids*, 167 (2012) 18.
19. J. Stygar, G. Żukowska and W. Wiczorek, *Solid State Ionics*, 176 (2005) 2645.

20. S. Selvasekarapandian, G. Hirankumar, J. Kawamura, N. Kuwata and T. Hattori, *Materials Letters*, 59 (2005) 2741.
21. C. Ramya, S. Selvasekarapandian, T. Savitha, G. Hirankumar and P. Angelo, *Physica B: Condensed Matter*, 393 (2007) 11.
22. J. Jurado, J. Trujillo, B.-E. Mellander and R. Vargas, *Solid State Ionics*, 156 (2003) 103.
23. M. S. A. Rani, N. A. Dzulkurnain, A. Ahmad and N. S. Mohamed, *International Journal of Polymer Analysis and Characterization*, 20 (2015) 250.
24. E. M. Sheha, M. M. Nasr and M. K. El-Mansy, *Journal of advanced research*, 6 (2015) 563.
25. M. S. A. Rani, A. Ahmad and N. S. Mohamed, *Polymer Bulletin*, 75 (2018) 5061.
26. M. Buraidah, L. Teo, S. Majid and A. Arof, *Physica B: Condensed Matter*, 404 (2009) 1373.
27. N.N. Mobarak, F. Jumaah, M. Ghani, M. P. Abdullah and A. Ahmad, *Electrochimica Acta*, 175 (2015) 224.
28. L. Ng and A. Mohamad, *Journal of Membrane Science*, 325 (2008) 653.
29. S. Rajendran, M. Sivakumar and R. Subadevi, *Materials Letters*, 58 (2004) 641.
30. M. S. A. Rani, N. H. Hassan, A. Ahmad, H. Kaddami and N. S. Mohamed, *Ionics*, 22 (2016) 1855.
31. R. N. Reddy and R. G. Reddy, *Journal of Power Sources*, 124 (2003) 330.
32. H. Hamsan, S. B. Aziz, M. Z. A. Kadir, M. Brza and W. O. Karim, *Polymer Testing*, (2020) 106714.

© 2021 The Authors. Published by ESG (www.electrochemsci.org). This article is an open access article distributed under the terms and conditions of the Creative Commons Attribution license (<http://creativecommons.org/licenses/by/4.0/>).